

# High-performance Multichannel Superconducting Single-Photon Detector System with Compact Cryocooler

Taro Yamashita, Shigehito Miki, and Hirotaka Terai

Advanced ICT Research Institute  
National Institute of Information and Communications  
Technology  
Kobe, Japan  
taro@nict.go.jp

Zhen Wang

Shanghai Institute of Microsystem and Information  
Technology  
Chinese Academy of Sciences  
Shanghai, China

**Abstract**—We present high-performance multichannel superconducting nanowire single-photon detector system with a compact Gifford-McMahon (GM) cryocooler. The best device showed a system detection efficiency (SDE) of 74%, dark count rate (DCR) of 100 cps, and full width at half maximum timing jitter of 68 ps at a bias current of 18.0  $\mu$ A. SDEs of 6 detectors mounted on the cryocooler were shown to be higher than 67% at the DCR of 100 cps.

**Keywords**—single-photon detector; superconductor; thin film; nanowire

## I. INTRODUCTION

Recently, superconducting nanowire single-photon detectors (SSPDs or SNSPDs) [1] have been studied actively as a promising candidate of single-photon detectors that can be applied in quantum information and communication technology, quantum optics, life science, classical laser communication technology, and light detection and ranging technology. The SSPDs potentially have broadband sensitivity that ranges from the visible to the near-infrared wavelengths, high system detection efficiency (SDE), low dark count rate (DCR), excellent timing resolution, and high counting rate [2]. The advantages of SSPD among single-photon detectors have been already demonstrated in applications to various research fields [3-6]. Further improvement of the system performance has been done, and especially in the practical applications, it is highly required to achieve high SDE, low DCR, and low timing jitter simultaneously.

Regarding the improvement of the SSPD system, extremely high SDE of 93% by using the tungsten silicide (WSi) nanowire has been reported by NIST group [7]. Although the obtained SDE certainly makes the WSi SSPDs attractive for use in various applications, the superconducting critical temperature ( $T_c$ ) of these films is extremely low to operate in Gifford-McMahon (GM) cryocooler systems while retaining their performances. MIT group demonstrated four-pixel

niobium nitride (NbN) SSPD array on thermally oxidized Si substrates in GM cryocooler system, and reported high system DE of 76%, low DCR of  $\sim 100$  cps, and timing jitter of 80 ps [8]. The authors also succeeded in showing the potential of their method to realize large-scale SSPD arrays. However, they used four-pixel array systems with a low temperature nanopositioner, which makes it highly complicated to realize independent, multichannel systems, required for specific applications such as quantum key distribution experiments. Furthermore, the switching current ( $I_{sw}$ ) reported in both paper was relatively small. The operation of SSPDs with a small  $I_{sw}$  is supposed to be unstable because of the contribution of the external environment (grounding noise, experimental setup connected to SSPD system, and more) to the fluctuation of the bias current's flow to the devices cannot be ignored. These detectors also require a cryogenic amplifier to achieve short timing jitter, making the cryocooler system complicated [7,8].

As an candidate of materials for SSPDs, niobium titanium nitride (NbTiN) can be adequate because its  $T_c$  is lower than that of NbN films, thus enabling higher detection efficiency of the SSPD system to absorbed photons [9,10]. On the other hand, the value of  $T_c$  is sufficiently higher than sample stage temperature of 2.3 K in GM cryocooler, enabling stable operation in GM cryocooler systems. In this work, we report the development of the high performance and multichannel NbTiN SSPD system with compact GM cryocooler, which is available for use in various applications. Our SSPD system has the following concomitant features that satisfy practical requirements and allow easy access from potential users. First, our detector system can achieve high SDE, low DCR, low timing jitter, and high  $I_{sw}$  at the same time. Second, our SSPD system uses fiber-coupled package technology, which is useful to achieve high optical coupling efficiency and install multi-packaged devices in a cryocooler system. Third, our system is based on compact GM cryocooler system with an operation temperature of 2.3K, which allows turnkey and continuous operation with low power consumption.

## II. MULTICHANNEL SSPD SYSTEM WITH COMPACT CRYOCOOLER

### A. Optical design and fabrication of device

Figure 1(a) shows the schematic structure of the fabricated NbTiN SSPD device. The structure of the cavity in this work was almost the same as the one that was reported in [8] as an effective structure to enhance the optical absorptance of photons in the NbTiN nanowire. In order to calculate the absorptance in this double-side cavity structure, we used the software PhotonicsSHA-2D in which one can model single-period multilayer gratings and simulate the electromagnetic behavior [11]. In this software, the incident wave enters the unit cell corresponding to the device with TE/TM polarization, and transmission as well as reflection can be calculated for an arbitrary wavelength range. In the simulation, we used complex refractive indices as  $n_{\text{Si}} = 3.63$ ,  $n_{\text{SiO}_2} = 1.44$ ,  $n_{\text{SiO}} = 1.551$ ,  $n_{\text{NbTiN}} = 4.563 + i4.911$ ,  $n_{\text{Ag}} = 0.322 + i10.99$  for Si substrate, SiO<sub>2</sub>, SiO, NbTiN, and Ag, respectively. These values were measured by the spectroscopic ellipsometry, and constant values at 1550 nm wavelength were used. The thickness of the SiO<sub>2</sub> (270 nm) and SiO (250 nm) layers were chosen to be  $\lambda/4$  for 1550-nm-wavelength incident light. The line and space of the NbTiN layer were assumed to be 100 nm and 60 nm, respectively. For the simplicity of the simulation, we assumed the incident light to be irradiated from the Si medium, and hence, light reflection from the back side of the Si substrate was not considered in the simulation. By performing the numerical simulation, we found that an excellent optical absorptance of 97% can be obtained at the wavelength of 1550 nm in this structure.

In the fabrication, we used the Si substrate in which the both surfaces were thermally oxidized to 270-nm-thick SiO<sub>2</sub> layers. The SiO<sub>2</sub> layer on the reserve side of the substrate functioned as an anti-reflection layer for 1550 nm wavelength and the layer at the front side functioned as a component of cavity structure. The NbTiN thin films that were used for the nanowire were deposited by DC reactive sputtering at an ambient substrate temperature [12]. We deposited 5-nm-thick NbTiN films and formed the film into a 100-nm-wide and 160-(200-) nm-pitch meandering nanowire that covered a square area of 15  $\mu\text{m} \times 15 \mu\text{m}$ . A 250-nm-thick SiO and a 100-nm-thick Ag mirror covered the nanowire to enhance the optical absorptance in the nanowire.

### B. Fiber-coupled package and cryocooler system

Here we briefly introduce our cryocooler systems reported in the previous papers [13,14]. As shown in Fig. 1(b), we adopted fiber-coupled compact packages that utilize fiber-spliced graded index (GRIN) lenses to realize the efficient optical coupling between incident photons and device active area [13]. The incident light is focused by GRIN lenses and the beam waist on the active area becomes around 9  $\mu\text{m}$ , which is smaller than the active area (15  $\mu\text{m} \times 15 \mu\text{m}$ ). After a careful alignment, the packaged devices were then installed into the GM cryocooler system with a 1.5 kW rated input power consumption at a driving frequency of 60 Hz (see Fig. 1(c)). This cryocooler system can cool the sample stage to 2.3 K, within thermal fluctuation of 10 mK. Further, it can set up to 6

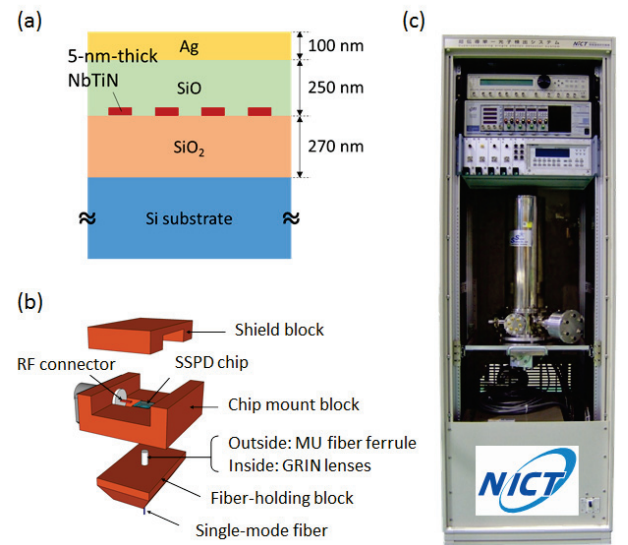


Fig. 1. (a) Schematic structure of the fabricated SSPD devices. (b) Fiber-coupled package for SSPDs. (c) Multichannel SSPD system with GM cryocooler.

SSPD packages for use in various applications that require several independent detector channels, such as quantum key distribution experiments [3-5]. The semi-rigid coaxial cables and single mode (SM) optical fibers for telecommunication wavelength were introduced into each package, and the optical fibers in a cryocooler system made several loops with a diameter of  $\sim 30$  mm to mitigate the dark counts that originated from the blackbody radiation [15]. The semi-rigid coaxial cables were connected to a bias tee and two room temperature low noise amplifiers at the outer side of the cryocooler.

## III. MEASUREMENT SETUP

Next we describe the measurement setup to evaluate the performance of the SSPD system. As performance factors of SSPD, we measured SDE, DCR, and timing jitter. In the measurements of SDE, we used a continuous tunable laser as an input photon source and input power was heavily attenuated by attenuator so that the photon flux at the input connector of the cryocooler was  $10^6$  photons/s which is sufficiently low to keep the linearity of the output counts to the incident photon flux. A fiber polarization controller was inserted in front of the optical input of the cryocooler in order to control the polarization of the incident photons so as to maximize SDE. In order to avoid the influence of periodic fringes resulting from the interference among the multi-optical layer boundaries, the wavelength of the incident photons was tuned to maximize the SDE in the range from 1540 to 1560 nm [16]. Although the optical losses from the input port to the device in our GM cryocooler system were confirmed to be 0.2 – 0.4 dB, these losses were not considered in the calibration of input photon flux. It is noted that these losses were mainly due to the fiber connector that was placed in the cryocooler system to simplify

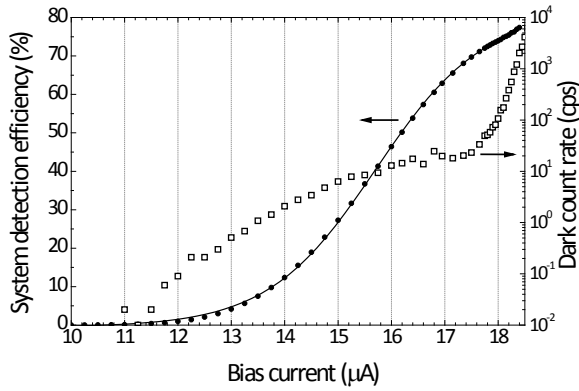


Fig. 2. Bias current dependences of the system detection efficiency (SDE, filled circles) and the dark count rate (DCR, open squares). Solid line indicates a fitting curve by the sigmoid function.

the detector exchanges, and could be easily improved by splicing the fibers. Consequently, SDE was obtained by subtracting DCR from the output count rate and by dividing this value by the input photon flux rate.

Regarding the timing jitter, we measured it by using the time-correlated single-photon counting (TCSPC) module with a 1 ps resolution (HydraHarp 400, PicoQuant GmbH). A 1550 nm wavelength pulsed laser with a 100-fs pulse width was used as the photon source and attenuated to be lower than 0.3 photons/pulse. The temporal correlations between the synchronized trigger pulses from pulsed laser module and the output pulses from the device through two room temperature low-noise amplifiers were recorded with the TCSPC module.

#### IV. SYSTEM PERFORMANCES

##### A. SDE and DCR

Figure 2 shows the bias current dependences of SDE and DCR of fabricated device (channel #1 in Table 1) with 100-nm-wide nanowire and 160-nm pitch. The  $I_{sw}$  of the device was 19.2 μA, which was sufficient to achieve stable operation. At the bias current close to  $I_{sw}$ , SDE reached maximal values of 77.3%, but this bias point may not be suitable for a practical use because of large DCR of around 10<sup>4</sup> cps. On the other hand, at the lower bias current of 18.0 μA, the device kept the high SDE of 74.0% with DCR of 100 cps, which makes it considerably attractive for use in various applications. As shown in Fig. 2, SDE clearly showed a sigmoid dependence on the bias current as reported in [17], we can use the method of least squares to derive the pulse generation probability after photon absorption to the nanowire,  $P_{pulse}$ . The solid curve in Fig. 2 indicates the obtained fitting curve, and the  $P_{pulse}$  was estimated to be 94.1%, when the current was biased close to  $I_{sw}$  even at 2.3 K.

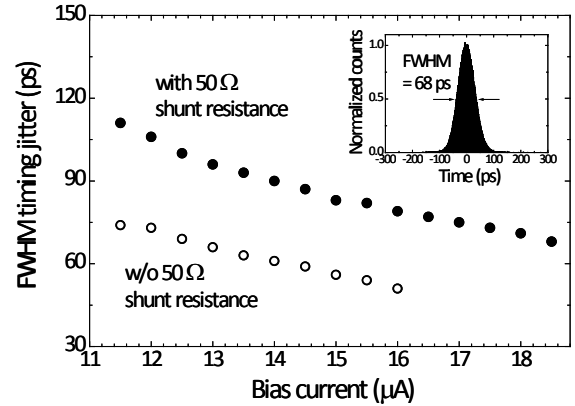


Fig. 3. Bias current dependences of the full width at half maximum (FWHM) timing jitter for the configuration with a shunt resistance (filled circles) and without a shunt resistance (open circles). Inset: The histogram of the time-correlated SSPD counts at the bias current of 18.0 μA with a 50 Ω shunt resistance.

As shown in Fig. 2, there are two different slopes in the bias current dependence of the dark counts, which caused by different physical origins [15]. For bias currents higher than ~17.5 μA, the dark counts are intrinsic one and mainly originate from the current-induced unbinding of vortex-antivortex pairs [18]. To avoid these intrinsic dark counts, the bias current dependence of SDE must have a saturated region so as to achieve the high SDE even for low bias current levels with no intrinsic dark counts. Although decreasing the operation temperature is simple and effective way to realize [15,18], a relatively large cooling system is necessary. Thus, it is preferable to achieve improvement in a way that does not require decreasing the operation temperature, for example, by optimizing superconducting characteristics and nanowire designs. On the other hand, the dark counts for bias currents lower than ~17.5 μA are caused by the blackbody radiation from the room temperature environment. We confirmed that this external DCR can be reduced less than around 1/10 without decreasing SDE, by making the fiber loops in a cryocooler. Insertion of effective band path filter would be necessary to further reduce DCR due to the blackbody radiation.

##### B. Timing jitter

We measured the timing jitter with two conventional readout configurations: one had a 50 Ω resistance connected in parallel to the device, and another had no shunt resistance. Figure 3 indicates the bias current dependences of the timing jitter defined as a full width at half maximum (FWHM) of time-correlated SSPD counts for both configurations. In the measurement, we used commercial room-temperature low noise amplifiers (LNA-550 and LNA-1000, RF Bay Inc.), which must have poorer performance than cryogenic amplifiers. Nevertheless, as shown in Fig. 3, we observed timing jitters

Channel	width/pitch (nm)	$T_c$ (K)			
#1	100/160	7.54	19.2	74.0	77.3
#2	100/160	7.49	20.6	73.0	76.6
#3	100/160	7.52	20.0	67.9	75.6
#4	100/200	7.48	18.2	67.0	71.7
#5	100/200	7.52	20.2	67.5	72.7
#6	100/200	7.52	19.8	67.3	71.0

Table 1. Summary of the nanowire design, superconducting characteristics, and the performances for six SSPD channels. SDE<sub>100DCR</sub> and SDE<sub>MAX</sub> indicate SDE at DCR of 100 cps and maximum SDE at the bias current close to  $I_{sw}$ , respectively.

that were lower than those reported in [7,8] because the present device has the high  $I_{sw}$ . In case that there is 50  $\Omega$  shunt resistance, the timing jitter was 68 ps at the bias current of 18.0  $\mu\text{A}$  where SDE and DCR were 74.0% and 100 cps, respectively (see the inset of Fig. 3). The shortest timing jitter of 51 ps was obtained at the bias current of 16.0  $\mu\text{A}$  without a shunt resistance. However, for the higher bias current without the shunt resistance, the device latched into the normal state and stopped functioning. Therefore, although the 50  $\Omega$  shunt resistance is indispensable to achieve the high SDE in this conventional readout configuration, new readout electronics aiming to avoid the latching in the high bias-current region without the 50  $\Omega$  shunt resistance would be effective. In fact, we have achieved a short timing jitter of 37 ps at a bias current value of 18  $\mu\text{A}$  for the device with similar  $I_{sw}$  to those in the present work, using single-flux-quantum readout circuit without latching near  $I_{sw}$  [19].

### C. Summary of performance for 6 channels

Toward the various applications, we have developed an SSPD system with 6 independent channels. Table 1 shows the summary of device designs, the superconducting characteristics, and SDEs of each channel. We used the devices with 100 nm width and 160 (200) nm pitch for the present SSPD system. Although the SSPDs with 100 nm width and 160 nm pitch showed slightly higher values than others, the SDEs of all channels were higher than 67% at DCR of 100 cps. Since  $I_{sw}$  of all devices showed similar values of around 20  $\mu\text{A}$ , the timing jitter values are expected to be comparably short, similar to those shown in Fig. 3.

## V. CONCLUSION

We have verified the performance of NbTiN SSPDs fabricated on a thermally oxidized Si substrate installed into compact fiber-coupled packages. We successfully demonstrated that the fiber-coupled packaged device, installed in a practical GM cryocooler system, simultaneously showed a SDE higher than 74.0% at a wavelength of 1550 nm, low DCR of 100 cps, and short timing jitter of 68 ps, at the large bias current of 18.0  $\mu\text{A}$ ; these values are significantly improved as compared to those reported in our previous works [13]. We also succeeded in building a practical SSPD system with 6

independent channels, and all channels showed SDE values higher than 67% at DCR of 100 cps, which can be instantly utilized for various applications. Ongoing studies aim to further improve the SDE, DCR, and timing jitter, for example, by improvement of optical absorptance in the nanowire, insertion of effective filter to cut the blackbody radiation, and improvement of the readout circuit to avoid latching behavior.

## ACKNOWLEDGMENT

The authors thank Saburo Imamura and Makoto Soutome of the National Institute of Communications Technology for their technical support. The authors also thank Mikio Fujiwara and Masahide Sasaki of the National Institute of Communications Technology for the fruitful discussions.

## REFERENCES

- [1] G. Gol'tsman, O. Okunev, G. Chulkova, A. Lipatov, A. Semenov, K. Smirnov, B. Voronov, A. Dzardanov, C. Williams, and R. Sobolewski, "Picosecond superconducting single-photon optical detector," *Appl. Phys. Lett.* **79**, 705 (2001).
- [2] C. M. Natarajan, M. G. Tanner, and R. H. Hadfield, "Superconducting nanowire single-photon detectors: physics and applications," *Supercond. Sci. Technol.* **25**, 063001 (2012).
- [3] H. Takesue, S. W. Nam, Q. Zhang, R. H. Hadfield, T. Honjo, K. Tamaki, and Y. Yamamoto, "Quantum key distribution over a 40-dB channel loss using superconducting single-photon detectors," *Nat. Photonics* **1**, 343 (2007).
- [4] M. Sasaki, M. Fujiwara, H. Ishizuka, W. Klaus, K. Wakui, M. Takeoka, S. Miki, T. Yamashita, Z. Wang, A. Tanaka, K. Yoshino, Y. Nambu, S. Takahashi, A. Tajima, A. Tomita, T. Domeki, T. Hasegawa, Y. Sasaki, H. Kobayashi, T. Asai, K. Shimizu, T. Tokura, T. Tsurumaru, M. Matsui, T. Honjo, K. Tamaki, H. Takesue, Y. Tokura, J. F. Dynes, A. R. Dixon, A. W. Sharpe, Z. L. Yuan, A. J. Shields, S. Uchikoga, M. Legre, S. Robyr, P. Trinkler, L. Monat, J.-B. Page, G. Ribordy, A. Poppe, A. Allacher, O. Maurhart, T. Langer, M. Peev, and A. Zeilinger, "Field test of quantum key distribution in the Tokyo QKD Network," *Opt. Exp.* **19**, 10387 (2011).
- [5] K. Yoshino, M. Fujiwara, A. Tanaka, S. Takahashi, Y. Nambu, A. Tomita, S. Miki, T. Yamashita, Z. Wang, M. Sasaki, and A. Tajima, "High-speed wavelength-division multiplexing quantum key distribution system," *Opt. Lett.* **37**, 223 (2012).
- [6] R. Ikuta, H. Kato, Y. Kusaka, S. Miki, T. Yamashita, H. Terai, M. Fujiwara, T. Yamamoto, M. Koashi, M. Sasaki, Z. Wang, and N. Imoto, "High-fidelity conversion of photonic quantum information to telecommunication wavelength with superconducting single-photon detectors," *Phys. Rev. A* **87**, 010301(R) (2013).
- [7] F. Marsili, V. B. Verma, J. A. Stern, S. Harrington, A. E. Lita, T. Gerrits, I. Vayshenker, B. Baek, M. D. Shaw, R. P. Mirin, and S. W. Nam, "Detecting Single Infrared Photons with 93% System Efficiency," *Nature Photonics* **7**, 210 (2013).
- [8] D. Rosenberg, A. J. Kerman, R. J. Molnar, and E. A. Dauler, "High-speed and high-efficiency superconducting nanowire single photon detector array," *Opt. Exp.* **21**, 1440 (2013).
- [9] S. N. Dorenbos, E. M. Reiger, U. Perinetti, V. Zwillaer, T. Zijlstra, and T. M. Klapwijk, "Low noise superconducting single photon detectors on silicon," *Appl. Phys. Lett.* **93**, 131101 (2008).
- [10] S. Miki, M. Takeda, M. Fujiwara, M. Sasaki, A. Otomo, and Z. Wang, "Superconducting NbTiN Nanowire Single Photon Detectors with Low Kinetic Inductance," *Appl. Phys. Exp.* **2**, 075002 (2009).
- [11] X. Ni, Z. Liu, F. Gu, M. G. Pacheco, J. Borneman, and A. V. Kildishev, "PhotonicsSHA-2D: Modeling of Single-Period Multilayer Optical Gratings and Metamaterials," <http://nanohub.org/resources/sha2d>. (DOI: 10.4231/D3WS8HK4X) (2012)

- [12] Z. Wang, S. Miki, and M. Fujiwara, "Superconducting Nanowire Single-Photon Detectors for Quantum Information and Communications," *IEEE J. Selected Topics in Quantum Electron.* **15**, 1741 (2009).
- [13] S. Miki, T. Yamashita, M. Fujiwara, M. Sasaki, and Z. Wang, "Multichannel SNSPD system with high detection efficiency at telecommunication wavelength," *Opt. Lett.* **35**, 2133 (2010).
- [14] S. Miki, M. Fujiwara, M. Sasaki, and Z. Wang, "Development of SNSPD System with Gifford-McMahon Cryocooler," *IEEE Trans. Appl. Supercond.* **19**, 332 (2009).
- [15] T. Yamashita, S. Miki, W. Qiu, M. Fujiwara, M. Sasaki, and Z. Wang, "Temperature Dependent Performances of Superconducting Nanowire Single-Photon Detectors in an Ultralow-Temperature Region," *Appl. Phys. Exp.* **3**, 102502 (2010).
- [16] S. Miki, M. Takeda, M. Fujiwara, M. Sasaki, and Z. Wang, "Compactly packaged superconducting nanowire single-photon detector with an optical cavity for multichannel system," *Opt. Exp.* **17**, 23357 (2009).
- [17] F. Marsili, F. Bellei, F. Najafi, A. E. Dane, E. A. Dauler, R. J. Molnar, and K. K. Berggren, "Efficient Single Photon Detection from 500 nm to 5  $\mu$ m Wavelength," *Nano Lett.* **12**, 4799 (2012).
- [18] T. Yamashita, S. Miki, K. Makise, W. Qiu, H. Terai, M. Fujiwara, M. Sasaki, and Z. Wang, "Origin of intrinsic dark count in superconducting nanowire single-photon detectors," *Appl. Phys. Lett.* **99**, 161105 (2011).
- [19] H. Terai, T. Yamashita, S. Miki, K. Makise, and Z. Wang, "Low-jitter single flux quantum signal readout from superconducting single photon detector," *Opt. Express* **20**, 20115 (2012).